Channeling of fast protons, deuterons, and α particles

O. N. Jarvis, A. C. Sherwood, and C. Whitehead
Nuclear Physics Division, A.E.R.E., Harwell, Didcot OX11 ORA, United Kingdom

M. W. Lucas
School of Mathematical and Physical Sciences, University of Sussex, Brighton BN1 9QH, United Kingdom
(Received 13 June 1978)

The ratios of channeled to random stopping powers have been obtained for light ions with $Z_1^2 E/M \simeq 160$ MeV travelling along the $\langle 110 \rangle$ and $\langle 111 \rangle$ axial directions, using a coincidence technique in which a silicon dE/dx detector was used as the channeling crystal. Dechanneling lengths $x_{1/2}$ and the trajectory spread contribution to energy loss straggling were also deduced from the dE/dx spectra. The concept of "best-channeled "particles is not applicable to experimental data obtained with targets of thickness $x \gtrsim x_{1/2}$. To compare experiment and theory, a first-order correction is made by averaging the valence-electron density distribution over the spread of trajectories permitted within the channel. Simple calculations are made which successfully reproduce the dechanneling lengths, trajectory spreads, and the stopping-power ratios for silicon. The simple formula for stopping-power ratios is then applied with equal success to the available high-energy data for germanium and is used to relate both silicon and germanium data to the existing quantum-theoretical treatments for "best-channeled" particles. The theory of Golovchenko and Esbensen gives good agreement with our deduced stopping powers for "best-channeled" particles.

I. INTRODUCTION

The problem of calculating the stopping powers for light ions in amorphous media, or for random incidence in crystalline media, was essentially solved by Bethe[1] and by Bloch[2] in the early 1930's. In recent years the calculation of the stopping power for ions incident along low-index directions of a single crystal has been tackled, but with inconsistent results. In particular, this situation persists even for the special case of high (but not relativistic) ion velocities, where the stopping is dominated by electron collisions. The work described here is the final experiment in a series designed to test the theoretical predictions[3,4] for the channeled stopping powers for high-velocity particles with special interest being devoted to protons as opposed to heavier ions. In the event, the observations made in the pursuit of a limited objective have resulted in a complete revision of our interpretation of the high-energy measurements.

In the previous experiments[5,6] the stopping powers for 160-MeV α particles channeled in silicon and in germanium have been measured by a difference technique using a Ge(Li) detector to obtain full-energy spectra; in this work it was found that the strong dechanneling made it advisable to restrict the target thickness to about 1 mm, producing a channeled energy loss of about 5 MeV, comfortably larger than the overall energy resolution of about 0.8 MeV. For 160-MeV protons the energy loss is only 0.5 MeV, and the best overall energy resolution available to us is 2.0 MeV, thus rendering the full energy difference technique impracticable. However, by using a silicon detector as the target measurements of the energy loss can be made directly in a manner which is insensitive to the energy spread of the incident beam. Such measurements have been made for 160-MeV protons, 85-MeV deuterons, and 160-MeV α particles.

In our earlier work, referred to above, we observed very good agreement between the experimental stopping-power ratios and the predictions obtained from the theory of Dettmann[3] and a clear disagreement with those from the theory of Golovchenko and Esbensen[4]; however, the latter authors (GE) appeared to be successful in predicting the stopping-power ratio for 700-MeV protons in germanium as determined by Esbensen *et al.*,[7] although the comparison here is between a nonrelativistic theory and a measurement at relativistic energies. This agreement we considered to be spurious because the statistical energy-loss straggling due to encounters with valence electrons had been incorrectly dismissed as negligible. The present experiment using 160-MeV protons shared with the experiment of Esbensen *et al.* the circumstance that the energy-loss distribution resulting from statistical fluctuations is highly skewed, at least for random orientation. This is not the case for our deuteron and α-particle data, which confirm our previous measurements and so validate the new technique. The skewness of the proton energy-loss spectra makes it necessary to establish a suitable valence-electron density for the straggling cal-

culation since for a skew distribution the mean energy loss is significantly greater than the most probable energy loss. It was this search for an averaged valence-electron density that led us to appreciate the inadequacy of the philosophy with which the high-energy channeling work has hitherto been approached. In the following account we find it convenient to reverse the chronological development and demonstrate how our present understanding of the high-energy channeling situation can be used to explain all our experimental observations.

The primary feature of our present understanding is simple and, in retrospect, obvious. It is that where a stopping-power measurement is made for channeled particles using a target thickness comparable with, or larger than, the dechanneling length, then there is no possibility of deducing directly from the energy-loss spectra the stopping power attributable to the "best-channeled" particles specified in most current theoretical treatments. Instead, allowance must be made for the smearing of particle trajectories resulting from multiple scattering due to the valence electrons. In the particular circumstances of our present and previous experiments it is appropriate to compute the averaged valence-electron density distribution using a straightforward procedure involving the entire lateral dimensions of the axial channels. At low energies where the circumstances permit more rigorous control of experimental detail, as in the work of Melvin and Tombrello,[8] the interpretation paradoxically becomes more difficult and recourse to a Monte Carlo method of analysis[9] may be necessary. The secondary feature of our present understanding is that it is possible to obtain an expression for the stopping-power ratio in the high-velocity limit that is both simple and compelling; while it cannot replace the need for a complete impact-parameter dependent quantum-theoretical calculation, our simple expression is arguably as accurate as the existing data and certainly more accurate than at least one of the published full-theoretical treatments.

II. EXPERIMENTAL

The Harwell synchrocyclotron was used to provide external beams of 85-MeV deuterons, 170-MeV α particles, or 160-MeV protons to the experimental area via a collimation system consisting of apertures of 2.5- and 1.0-mm diameter separated by 7.5 m in an evacuated beam pipe with thin entrance and exit windows. The silicon detector which served as the target was mounted in a goniometer, in air. After passing through the detector the particle beam entered another evacuated pipe and was directed onto a third collimator (1.0 mm diameter) placed in front of a thin-window Ge(Li) detector. The Ge(Li) detector provided a timing signal to gate the silicon detector such that the ΔE signals recorded were mainly those due to channeled particles, a feature which takes advantage of the reduced multiple scattering of channeled particles as compared with those possessing unaligned trajectories.

The silicon detector was 0.739 ± 0.006 mm thick, cut with its $\langle 111 \rangle$ axis very nearly normal to its surface and held in a triple-axis goniometer controlled by stepping motors with step size corresponding to 0.01°. Movement between the $\langle 111 \rangle$ and $\langle 110 \rangle$ directions was obtained by turning the silicon target through 35°16′ along the $\{110\}$ plane. The approximate channeling alignment was obtained by optimizing the channeled fraction of the α-particle energy spectrum recorded in the Ge(Li) detector. This procedure was merely a repetition of the earlier experiments[5,6]; the Ge(Li)-detector thickness was sufficient to stop α particles but not deuterons or protons. Random target alignment was obtained by rotating the target through just 1° so as to minimize the increase in thickness of target presented to the beam while taking care to avoid channeling planes. Once the target alignment had been determined with the α-particle beam, the deuteron or proton beams could then be acquired, with final minor adjustments being made using the silicon detector ΔE spectra for channeled particles as a guide (a tedious exercise because of the coincidence requirement).

Figures 1–6 show typical dE/dx spectra for α particles, deuterons, and protons for $\langle 110 \rangle$ and $\langle 111 \rangle$ axial directions in silicon, with results for aligned and random orientations of the target superimposed. The coincidence requirement between the two detectors is important because the data analysis is concerned more with the mean-energy loss of the channeled fraction than with the position of the low-energy loss leading edge intercept, and only the latter can be determined from the singles spectra. The relative strength of the channeled fraction of each aligned spectrum is sensitive to the accuracy with which the target is aligned, to the degree of collimation used and to the amount of multiple scattering suffered by the beam before entering the target. This is to be expected since the channeling acceptance angle ψ_1 is typically only 0.06°, where ψ_1 is the angle defined by Lindhard $\psi_1 = (2Z_1 Z_2 e^2/Ed)^{1/2}$ in which Z_1 and Z_2 refer to the incident particle and the target atoms, E is the energy of the incident particle and d is the interatomic spacing along the

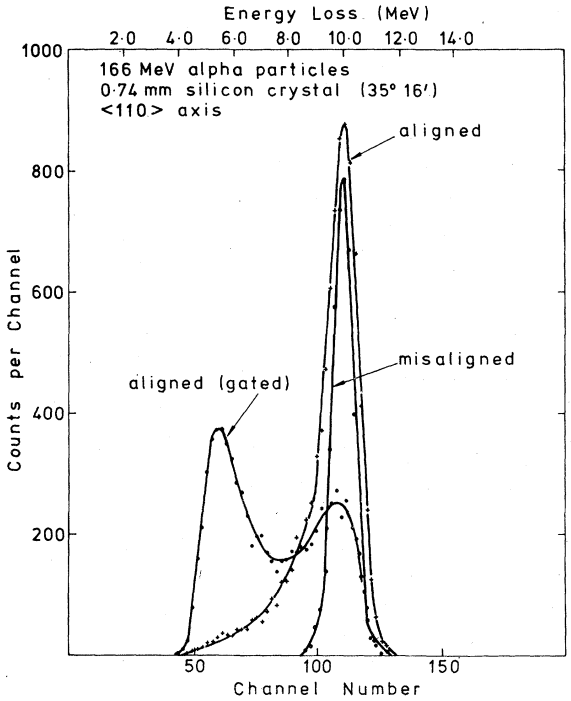

FIG. 1. Si ΔE counter-energy spectra for 166-MeV α-particles. Singles spectra are shown for the detector aligned, with its ⟨110⟩ axis parallel to the incident beam, and for a slight misalignment. The coincidence spectrum (gated) is shown for alignment only. The solid lines are drawn only to guide the eye.

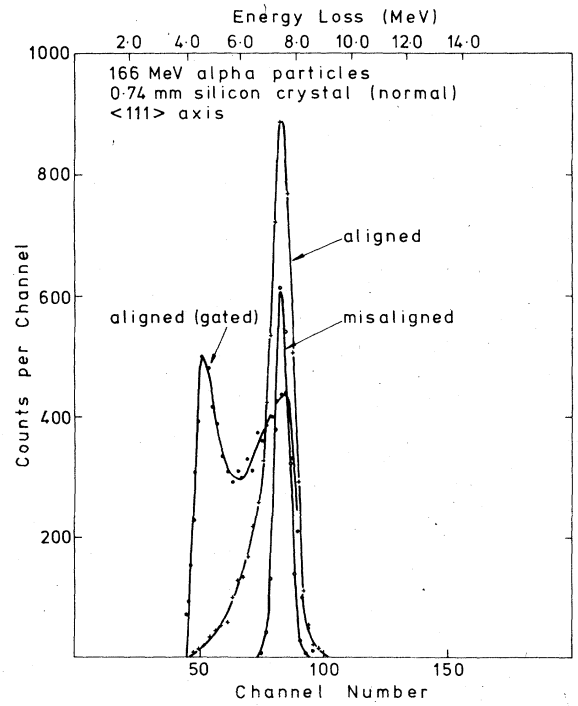

FIG. 2. Same as Fig. 1, for 166-MeV α particles and the ⟨111⟩ axis.

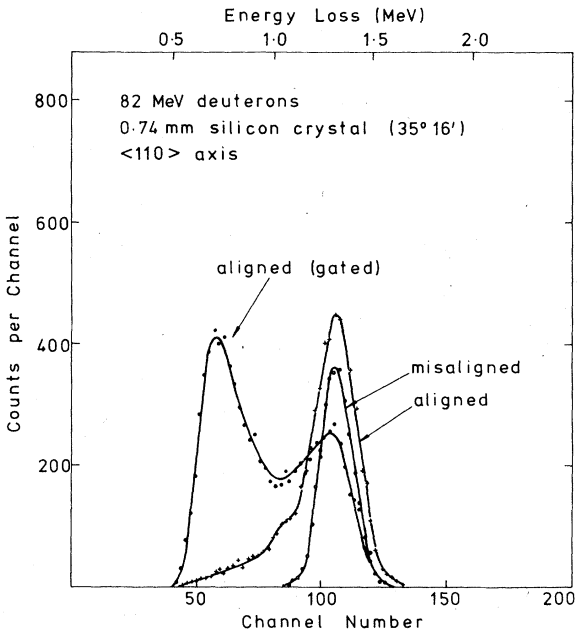

FIG. 3. Same as Fig. 1. for 82-MeV deuterons and the ⟨110⟩ axis.

row. Of importance for the interpretation of the data is the fact that the position of the leading edge intercept—the most readily monitored feature—was independent of target orientation for misalignments of at least 0.06° and, moreover, was independent of beam intensity for all reasonable counting conditions.

The electronic amplification system used with

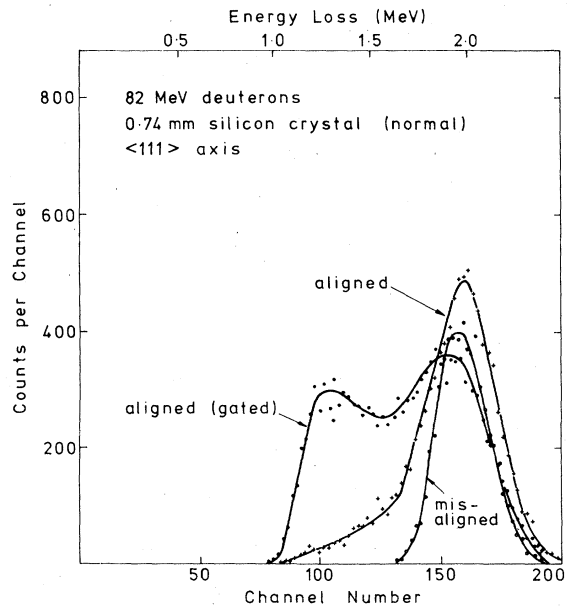

FIG. 4. Same as Fig. 1 for 82-MeV deuterons and the ⟨111⟩ axis.

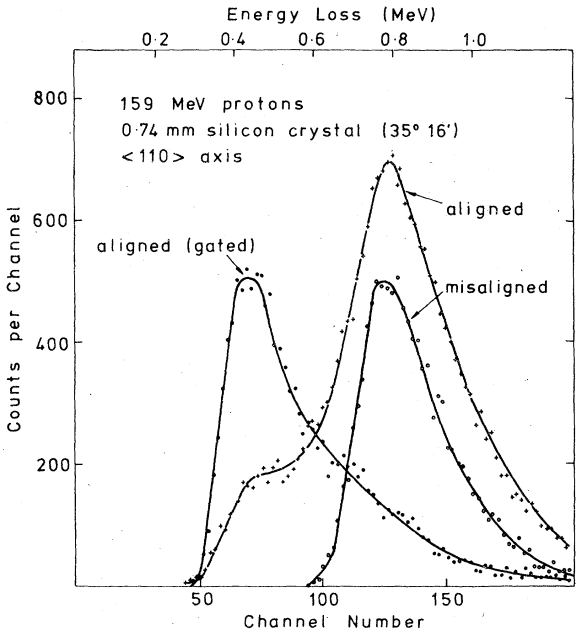

FIG. 5. Same as Fig. 1, for 159-MeV protons and the ⟨110⟩ axis.

the silicon detector incorporated double sampling to cancel the effects of base-line disturbance and to reject any overlapping pulses by the application of carefully designed paralysis times. Such a system was necessary because while our coincidence counting rates were only of the order of

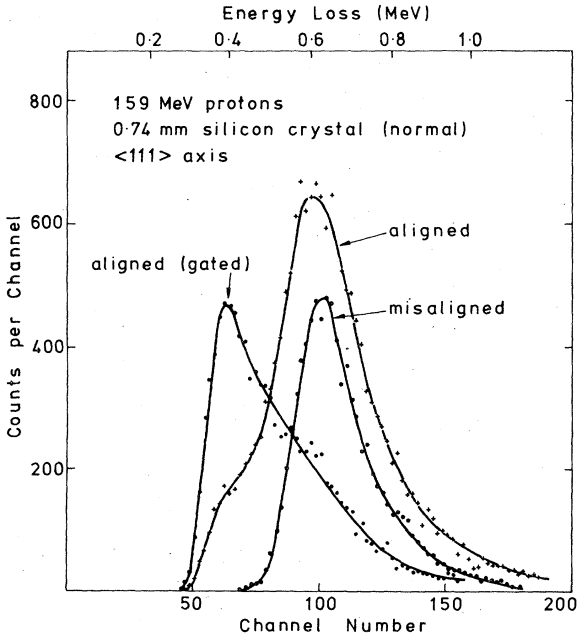

FIG. 6. Same as Fig. 1, for 159-MeV protons and the ⟨111⟩ axis.

1 Hz the silicon ΔE detector singles rates were nearly 1 kHz which, because of the synchrocyclotron duty-cycle factor of a few percent, implies very high instantaneous counting rates. However, no degradation of the energy resolution due to counting-rate effects was observed during the data-taking period. The detector noise was about 30 keV and was not expected to be significant for the present work, but during the course of the analysis, it became clear that the channeled spectra could be fitted theoretically only if the energy resolution was apparently degraded as, for example, by the application of a Gaussian noise distribution with full width at half maximum (FWHM) considerably in excess of 30 keV. That this broadening did not have an explanation in terms of a counting-rate effect was demonstrated by arranging for the precision pulser to inject a test signal into the ΔE preamplifier during the beam burst, at times controllable relative to the start of the beam burst. The same pulser signal was also fed to the Ge(Li) detector so that the normal coincidence arrangement was effective. No increase in the noise level was observed even for beam intensities which overwhelmed the silicon detector; this is no more than would be expected from an electronic processing system which rejects all dubious events. No instrumental explanation for the broadening could be found and it was eventually appreciated that the effect is intrinsic to the channeling process, as will be discussed later.

In the present work our major concern was to determine the ratios of the channeled stopping power to the random stopping power for the three light ions so that it was not necessary to make a precise energy calibration of the detector and, consequently, the energy scales shown in the figures were derived from stopping power tables. In a subsequent measurement the detector was calibrated using an ^{241}Am α-particle source, and the random-energy loss for α particles was again determined, resulting in a stopping power of 1.084 ± 0.010 eV/Å for 160-MeV α particles in silicon—in excellent agreement with the tabulation of Bichsel and Tschalär,[10] which gives 1.082 eV/Å.

When a silicon or other detector is used as the specimen for a stopping power measurement it should be appreciated that the quantity measured is the number of ion pairs produced by the passage of the incident particle and that this number, although proportional to the energy loss, may not be the same for channeled as for random trajectories. In the present paper we assume that the number of ion pairs per unit energy loss for channeled particles is precisely the same as for

particles travelling in a random direction. This is justifiable because, as described elsewhere,[11] we have been able to demonstrate equality to an accuracy of 2% for 160-MeV α particles in silicon.

III. THEORY

In the present experiment we are concerned with the transport of fast, light ions along a major crystallographic axis in a single crystal and we observe the three quantities (i) stopping power, (ii) multiple scattering—in particular as it affects particle dechanneling, and (iii) energy loss straggle due to statistical fluctuations and to trajectory spread. Because of the relatively thick target we were obliged to use, our channeling description emphasizes features which, although still present, tend to be ignored in low-energy experiments. We begin our analysis with a brief review of the three observable quantities with reference to a random system such as amorphous material or a crystal in which the particle beam is constrained to avoid the crystallographic planes and axes. Further details of the relevant formulae as applied to a low-energy experiment can be found in the paper of Melvin and Tombrello[8] and in the review article of Gemmell.[12] With this background the channeling situation is easily developed.

A. The random system: general formulae

For a random arrangement of atoms the stopping power has been treated by Bethe[1] and by Bloch[2] in terms of contributions from scattering by nuclei and by electrons. The nuclear contribution is

$$\left(\frac{dE}{dx}\right)_n=\left(\frac{4\pi Z_1^2Z_2^2e^4}{M_2v^2}\right)N\ln\left(\frac{1.29aM_2E}{Z_1Z_2(M_1+M_2)e^2}\right), \quad (1)$$

where Z_1, M_1 and Z_2, M_2 are the atomic numbers and masses of the projectile and target atoms, v is the projectile velocity and E its energy, N is the number of target atoms per unit volume, and the screening distance a is the Thomas-Fermi radius $0.4685\ Z_2^{-1/3}$ Å. The electronic contribution is

$$\left(\frac{-dE}{dx}\right)_e=\left(\frac{4\pi Z_1^2e^4}{mv^2}\right)NZ_2\ln\left(\frac{2mv^2}{I}\right), \quad (2)$$

where m is the electron mass and I is a mean ionization potential, which is determined empirically to be about $11Z_2$ eV (in practice we use 172 eV for silicon, 343 eV for germanium). For fast, light ions the collisional energy loss is transferred predominantly to electrons, i.e.,

$$\left(\frac{-dE}{dx}\right)_e\gg\left(\frac{-dE}{dx}\right)_n.$$

As we are interested in the ratios of stopping powers, it is convenient to concentrate on the factor $Z_2\ln(2mv^2/I)$. In the special case of an electron gas in which the electron density is nonuniform the factor $Z_2\ln(2mv^2/I)$ can be split[13] into two terms, $Z\ln(v/v_F)+Z_{\text{loc}}\ln(2mvv_F/\hbar\omega)$. This separation follows from an integration cutoff determined by the ratio ω/v_F, where $\hbar\omega$ is the plasmon energy, and v_F is the Fermi velocity of the electron gas:

$$\hbar\omega=\hbar(4\pi e^2NZ/m)^{1/2}; \quad (3)$$

$$v_F=\hbar(3\pi^2NZ)^{1/3}/m. \quad (4)$$

The first term is attributable to collective or plasmon excitations and depends on the average electron density since the interaction is of long range. The second term is due to single particle excitations, involving high-momentum transfers, and depends only on the local density. Note that for an electron gas of uniform density $Z=Z_{\text{loc}}$ and the two logarithmic terms sum to give $Z\ln(2mv^2/\hbar\omega)$.

The energy-loss distribution for a monokinetic ion beam that has passed through a very thin target is given by the Landau-Vavilov calculation,[14] which makes allowance for the statistically small number of collisions. For relatively thick targets, where Poisson statistics may be applied, the energy-loss distribution becomes Gaussian with a width determined by

$$\frac{d(\Delta E)^2}{dx}=4\pi Z_1^2e^4NZ_2 \quad (5)$$

and is due to high-momentum-transfer collisions with the target electrons (i.e., $Z_2=Z_{\text{loc}}$). For very thick targets the energy-loss distribution again becomes skewed and the representation of Tschalär[15] should be used.

The multiple scattering suffered by an ion in amorphous material is determined by ion-nucleus collisions since the momentum transfer to a nucleus is much larger than that to an electron (although the mean energy transfer is far less), i.e.,

$$\left(\frac{d\Omega^2}{dx}\right)_n\gg\left(\frac{d\Omega^2}{dx}\right)_e.$$

Expressed in terms of stopping powers, we have

$$\left(\frac{d\Omega^2}{dx}\right)_n=\frac{M_2}{M_1E}\left(\frac{-dE}{dx}\right)_n \quad (6)$$

and

$$\left(\frac{d\Omega^2}{dx}\right)_e=\frac{m}{2M_1E}\left(\frac{-dE}{dx}\right)_e, \quad (7)$$

where the factor $\frac{1}{2}$ for electron multiple scattering is an approximate allowance for the fact that only close collisions with electrons contribute; more accurately, we have

$$\left(\frac{d\Omega^2}{dx}\right)_e = \frac{m}{M_1 E}\left(\frac{-dE}{dx}\right)_{e,\text{close}} = \frac{m}{M_1 E}\left(\frac{4\pi Z_1^2 e^4}{mv^2}\right) N Z_2 \ln\left(\frac{2mvv_F}{\hbar\omega}\right), \quad (8)$$

where $Z_2 = Z_{1oc}$.

B. Channeling: stopping-power ratios

The above formulae have been displayed in a manner which permits a straightforward application to the situation experienced by channeled particles, in which the stopping power, energy-loss straggling and multiple scattering are reduced because of the suppression of all close collisions with atoms. For random stopping the product $Z_2 \ln(2mv^2/I)$ can be written as before in terms of close and distant collisions, but distinguishing in addition between valence and the bound core electrons, we write

$$Z_2 \ln\left(\frac{2mv^2}{I}\right) = 4\ln\left(\frac{2mvv_F}{\hbar\omega}\right) + 4\ln\left(\frac{v}{v_F}\right) + (Z_2 - 4)\ln\left(\frac{2mvv_F}{\hbar\omega}\right) + (Z_2 - 4)L_{c,d}, \quad (9)$$

where we recognize the existence of four valence electrons for silicon and germanium (which exist as an electron gas), where the electron binding energy is considered to have an insignificant effect on the close-encounter stopping contribution for very high-velocity particles and where the factor $L_{c,d}$ represents the contribution of the core electrons to the distant collision loss. For channeled particles the valence electron contribution must take into account the nonuniform distribution of valence electrons across the channel, the close collisions with core electrons should be totally suppressed and the distant collision term for core electrons should be approximately equal to that for random collisions, at least for low-Z_2 atoms and high-particle velocities; on this latter point Dettmann[3] specifically comments that 160-MeV protons channeled in silicon contribute to the "low excitation" of ion cores with an efficiency comparable with random conditions. With the stopping ratio $R_{\langle hkl\rangle}$ defined as

$$R_{\langle hkl\rangle} = \frac{(-dE/dx)_{\text{ch}}}{(-dE/dx)_r} = \frac{\langle Z_2 L_e\rangle_{\text{ch}}}{\langle Z_2 L_e\rangle_r}, \quad (10)$$

we have for channeled particles

$$R_{\langle hkl\rangle} Z_2 \ln\left(\frac{2mv^2}{I}\right) = Z_{1oc}\ln\left(\frac{2mvv_F}{\hbar\omega}\right) + 4\ln\left(\frac{v}{v_F}\right) + (Z_2 - 4)L_{c,d}. \quad (11)$$

On eliminating the term $L_{c,d}$ a relationship between $R_{\langle hkl\rangle}$ and Z_{1oc} is displayed:

$$R_{\langle hkl\rangle} = 1 - \frac{(Z_2 - Z_{1oc})}{Z_2}\,\frac{\ln(2mvv_F/\hbar\omega)}{\ln(2mv^2/I)}. \quad (12)$$

The above relationship is appropriate for nonrelativistic energies and should be adequate for the data presented here, for which the relativistic intrusion is slight, but we will also wish to apply it to the conditions of Esbensen *et al.*, which are unashamedly relativistic; the formula used hereafter is therefore

$$R_{\langle hkl\rangle} = 1 - \frac{(Z_2 - Z_{1oc})}{Z_2} \times \frac{\ln(2mvv_F/\hbar\omega) - \ln(1-\beta^2)^{1/2} - \frac{1}{2}\beta^2}{\ln(2mv^2/I) - \ln(1-\beta^2) - \beta^2 - \frac{1}{2}\delta}, \quad (13)$$

where $\frac{1}{2}\delta$ is the small-density effect correction to the distant collision term, important only for $\beta = v/c \approx 1$. For best-channeled particles Z_{1oc} is just the electron density at the center or axis of the channel, Z_{axis}. For less-well-channeled particles Z_{1oc} will be obtained by taking an average over the electron density distribution. For trajectories which extend into the channel walls it is probable that the outer core electrons will make a small contribution to the stopping due to close collisions; this enhancement can be considered to be included in Z_{1oc}.

From our previous 160-MeV α particle experiment with silicon we have $R_{\langle 110\rangle} = 0.499 \pm 0.021$ and $R_{\langle 111\rangle} = 0.615 \pm 0.013$. From these results we deduce $Z_{1oc,\langle 110\rangle} = 4.9 \pm 0.4$ and $Z_{1oc,\langle 111\rangle} = 7.0 \pm 0.4$. Applying these Z_{1oc} values for 85-MeV deuterons [Eq. (13)] leads us to expect the same ratios $R_{\langle hkl\rangle}$ as for α particles, while for 160-MeV protons, we would predict small increases to $R_{\langle 110\rangle} = 0.54 \pm 0.02$ and $R_{\langle 111\rangle} = 0.64 \pm 0.02$.

The values we have deduced for Z_{1oc} are rather high in relation to those considered appropriate in low-energy channeling experiments. Of particular interest is the work of Melvin and Tombrello[8] (MT) in which stopping-power measurements were made for protons channeled in silicon at energies sufficiently low (0.6 to 1.6 MeV) that only the valence electrons contribute to the channeled stopping. In deference to the familiar uncertainty as to whether the best-channeled stopping power is to be derived from the peak or the extrapolated leading edge of the energy-loss spectrum MT extracted values of Z_{1oc} appropriate

to each; however, they point out that because of energy-loss straggling the best-channeled stopping power will fall between these two extremes—this is correct, as will be apparent later, only because the dechanneling is negligible. Experimentally, MT have thus determined $Z_{1oc}=Z_{axis}$ to lie in the ranges

$$1.1\pm0.4<Z_{axis,\langle 110\rangle}<2.9\pm0.5$$

and

$$2.8-3.8\pm0.7<Z_{axis,\langle 111\rangle}<4.5-5.2\pm0.8\,.$$

They also obtained theoretical estimates for Z_{axis} by expressing the sum of the row averaged Thomas-Fermi potentials in quartic form for small displacements r from the axis, $V(r)=V_0r^2+V_1r^4$, and then solving the Poisson equation $\nabla^2V(r)=4\pi eZ_{1oc}(r)$. Correcting a minor slip concerning the use of spherical or cylindrical variables, the resulting Z_{axis} values are $Z_{axis,\langle 110\rangle}=1.51$ and $Z_{axis\langle 111\rangle}=3.00$. Desalvo and Rosa[9] have recently published the results of a dielectric calculation of stopping powers that incorporated a Monte Carlo simulation of the ion trajectories which are influenced by electron multiple scattering and the valence electron density distribution; their results correspond to the average energy loss and should be compared with the peak values of MT. Excellent agreement is found between theory and experiment for both axial and planar channeling; in particular they compute $Z_{1oc,\langle 110\rangle}=2.72$ and $Z_{1oc,\langle 111\rangle}=3.00$.

Thus far it may appear that not only are the values for Z_{1oc} deduced from Eq. (13) of possibly suspect provenance, but that they are far too high, being double those calculated by Desalvo and Rosa. However, there are qualitative differences between the low- and high-energy experiments which can best be illustrated by calculating the wavelength λ with which particles travelling along a channel undergo oscillations about the channel axis. For modest values of the transverse energy $E_\perp=E\psi^2$ the wavelength for a particle which crosses the axis is easily found to be

$$\lambda=4\int_0^{r_m}\left(\frac{E}{E_\perp-V(r)}\right)^{1/2}dr\,, \tag{14}$$

where r_m is the amplitude of the oscillation and $V(r)\simeq V_0r^2$ for the central region of the channel. Thus, $\lambda=2\pi(E/V_0)^{1/2}$, where V_0 is known from MT to be 3.35 (6.67) eV/Å^2 for the $\langle 110\rangle$ ($\langle 111\rangle$) axes. At 1.6 MeV the wavelength $\lambda\sim0.3$–0.4 μm, which is comparable with the target thickness (1 μm) used by MT, whereas at 160 MeV we find $\lambda\sim3$–4 μm, which is very short compared with the target thickness of nearly 1000 μm demanded by experimental considerations. Thus, at low energies the transmitted particle will experience a valence electron density essentially determined by the initial displacement r_0 on entry into the channel, whereas at high energies all accessible regions of the channel will be explored as permitted by $E_\perp$. A further difference is that when the electron multiple scattering is important, as it will be for thick targets, all knowledge of the value of the transverse energy acquired on entering the crystal $E_\perp(x=0)$ will be lost after a small penetration x and the $E_\perp$ values for all particles will cluster more or less closely around some expectation value $\langle E_\perp(x)\rangle$ to which there will be a corresponding $\langle Z_{1oc}(x)\rangle$.

C. Averaged electron density for channeling

Lindhard[16] has shown for axially channeled particles that the probability of finding a particle with transverse energy $E_\perp$ at any position within the accessible area is independent of that position once the particle has penetrated a distance sufficient for statistical equilibrium to have been reached. The probability distribution is

$$P_0(E_\perp,r)=\begin{cases}\dfrac{1}{A(E_\perp)}, & E_\perp>V(r)\\ 0 & E_\perp<V(r)\end{cases}, \tag{15}$$

where $A(E_\perp)$ is the area accessible to a particle moving in the potential $V(r)$. For a well-collimated particle beam the initial ($x=0$) population of transverse energies will be peaked strongly around $E_\perp=0$. With increasing penetration the population distribution will broaden due to the diffusion of $E_\perp$ values resulting from electron scattering encounters in a manner best determined by having recourse to Monte Carlo methods. For the high-energy experiments considered here, the divergence of the beam entering the detector was comparable with the critical channeling angle $\psi_c\approx\psi_1$ so that the initial population was essentially flat from $E_\perp=0$ to the maximum value consistent with channeling $E_\perp=E\psi_c^2$, and will remain so provided dechanneling can be neglected. For a uniform $E_\perp$ distribution the calculation of an averaged electron density is straightforward.

For the case of an isolated atomic row, the continuum potential at a distance ρ is

$$U(\rho)=E\psi_1^2(\rho/a)\,. \tag{16}$$

Using the Molière screening function, a good analytical approximation to the Thomas-Fermi screened ion-atom potential, we find

$$U(\rho)=\frac{2Z_1Z_2e^2}{d}\left[0.10K_0\left(\frac{6\rho}{a}\right)+0.55K_0\left(\frac{1.2\rho}{a}\right)+0.35K_0\left(\frac{\rho}{a}\right)\right], \quad (17)$$

where K_0 is the reduced Hankel function of order zero. The total potential $V(y,z)$ is obtained by summing contributions from nearby strings, not just those defining the channel. The local charge density $Z_{\rm loc}(y,z)$ is obtained by solving the Poisson equation; contour plots of the electron density for ⟨110⟩ and ⟨111⟩ channels in silicon and germanium are shown in Figs. 7–10. For a particular transverse energy, the averaged charge density is evidently

$$Z_{\rm loc}(E_\perp)=\frac{1}{A(E_\perp)}\int\int Z_{\rm loc}(y,z)\,dy\,dz\,, \quad (18)$$

where the upper limits of integration are defined by $E_\perp=V(y,z)$ or the dimensions of the channel. Since the transverse energy distribution is uniform, the full average becomes

$$\langle Z_{\rm loc}\rangle=\int_0^{E\psi_c^2} Z_{\rm loc}(E_\perp)\,\frac{dE}{E\psi_c^2}\,. \quad (19)$$

The critical channeling angle is given by

$$\psi_c=[f(\rho_c/a)]^{1/2}\psi_1\,,$$

where ρ_c is the closest distance of approach to a row compatible with sustaining a stable channeling trajectory. Unfortunately, ρ_c is not known

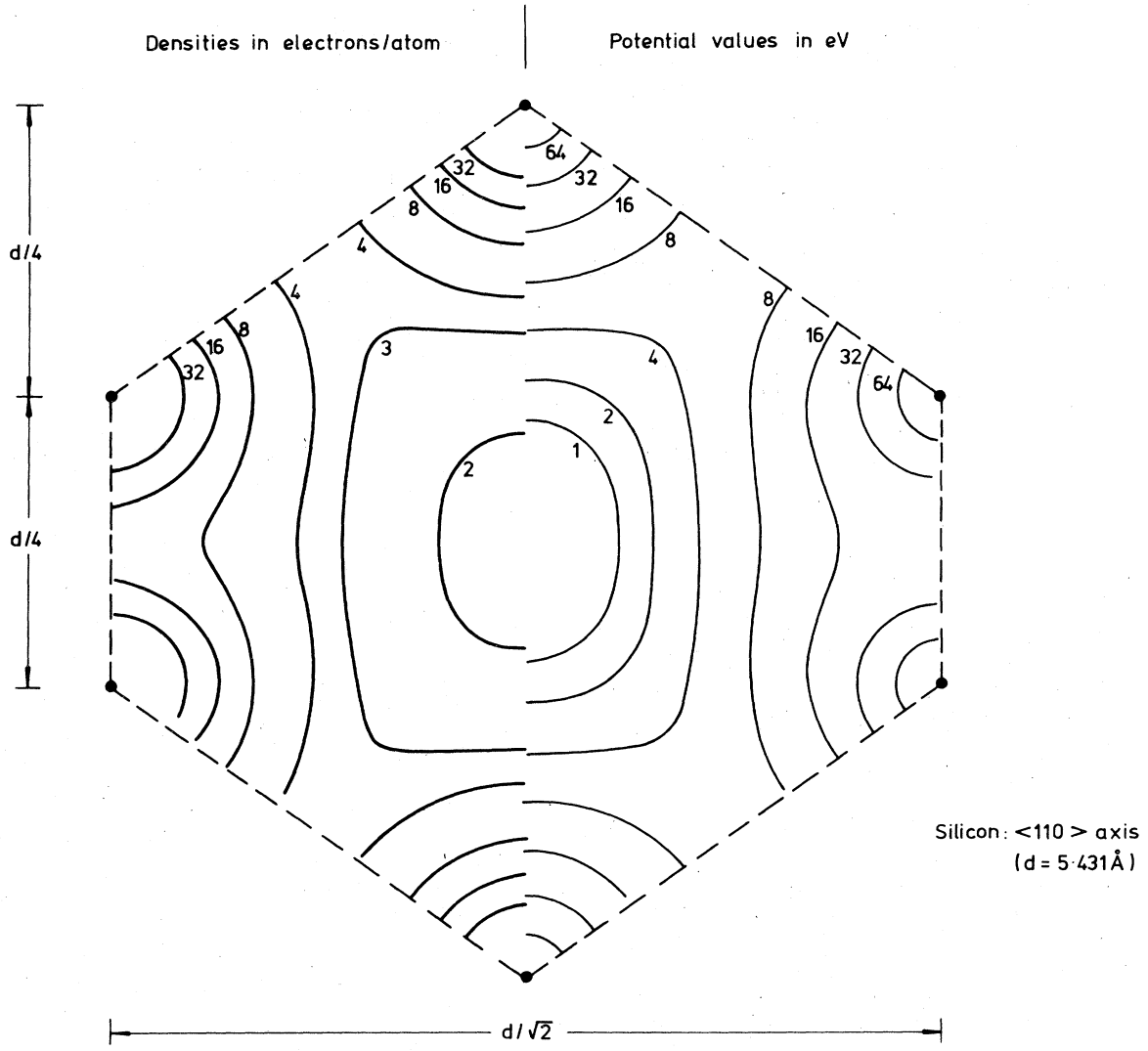

FIG. 7. Equicontour lines of the net continuum potential for protons (thin lines on the right) and the corresponding local electron density (thick lines on the left) in the {110} transverse plane of silicon. The potential values are in eV and the densities in electrons per atom. The spacing of atoms along the axis is given by $d/\sqrt{2}$.

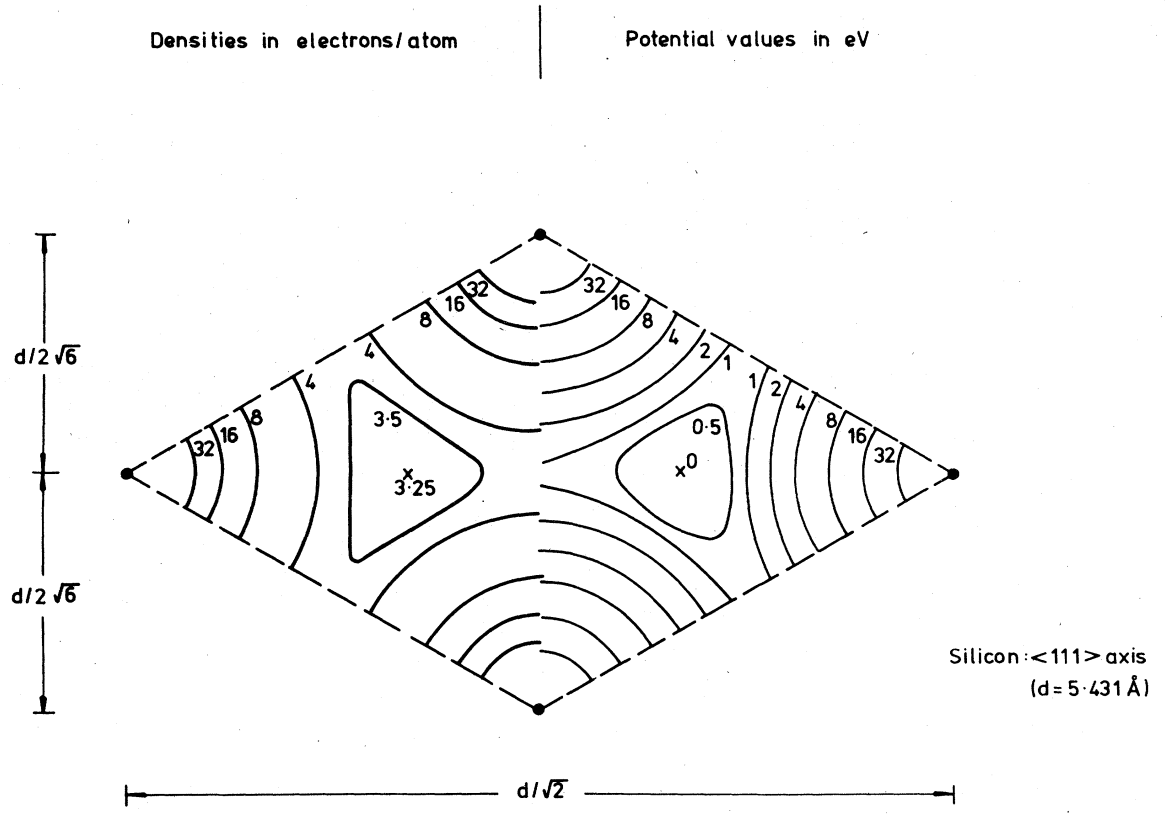

FIG. 8. Same as Fig. 7, for the {111} transverse plane in silicon. The atoms are separated along the axis alternately by $d\sqrt{3}/4$ and $d3\sqrt{3}/4$.

precisely, although the Lindhard estimate $\rho_c \approx a$ yields $\psi_c = 0.83\psi_1$. For a flat $E_\perp$ distribution there should be no difference between ψ_c and the half angle $\psi_{1/2}$, which is the quantity usually determined experimentally.[12] Barrett[17] has found the formula

$$\psi_{1/2}(\text{Barrett}) = 0.80[f(1.2u_1/a)]^{1/2}\psi_1 \qquad (20)$$

to give a good representation of a wide range of measurements taken at low energies with thin targets (~ 1 μm); u_1 is the thermal vibration amplitude. The limited information for high energies[7,18] shows

$$\psi_{1/2}(\text{obs}) = (0.56 \pm 0.04)\psi_{1/2}(\text{Barrett}), \qquad (21)$$

although the Barrett value does give a good fit to the half-width at the mouth of the channeling dip. The measured half angle is expected to fall as the target thickness increases because of the loss of particles with large ψ by dechanneling, so the Barrett formula should really be applied to $\psi_{1/2}$ extrapolated to zero thickness. For very thick targets an equilibrium $E_\perp$ distribution should be achieved. This is demonstrated in the measurements by Acerbi[18] for 38.9 MeV protons channeled in silicon where $\psi_{1/2}$ was observed to remain constant over the target thickness range 60–1500 μm. There is reason, therefore, for adopting the Barrett formula at high energies for very thin targets, thus determining the maximum divergence angle for particles initially accepted for channeling, and also as defining the critical angle at which particles are subsequently dechanneled.

Although it is reasonable to take $\psi_c = \psi_{1/2}$ (Barrett) [henceforth use (B) for (Barrett)] it is evident that $E\psi_c^2$ is not the appropriate maximum transverse energy for our electron density averaging procedure, since the $E_\perp$ distribution is not flat. The channeling dip measurements[7,18] are compatible with a trapezoidal distribution in ψ, defined by a base width of 2 $\psi_{1/2}$(B) and a FWHM of twice $0.56\psi_{1/2}$(B). This distribution is readily converted into an $E_\perp$ distribution which we have used in our calculations for $\langle Z_{1oc}\rangle$. The resulting $\langle Z_{1oc}\rangle$ estimates fall approximately midway between estimates derived from flat distributions with $E_\perp(\text{max}) = E\psi_{1/2}^2(\text{obs})$ and $E\psi_{1/2}^2(\text{B})$. We arbitrarily assign uncertainties to $\langle Z_{1oc}\rangle$, corresponding to one quarter the difference between

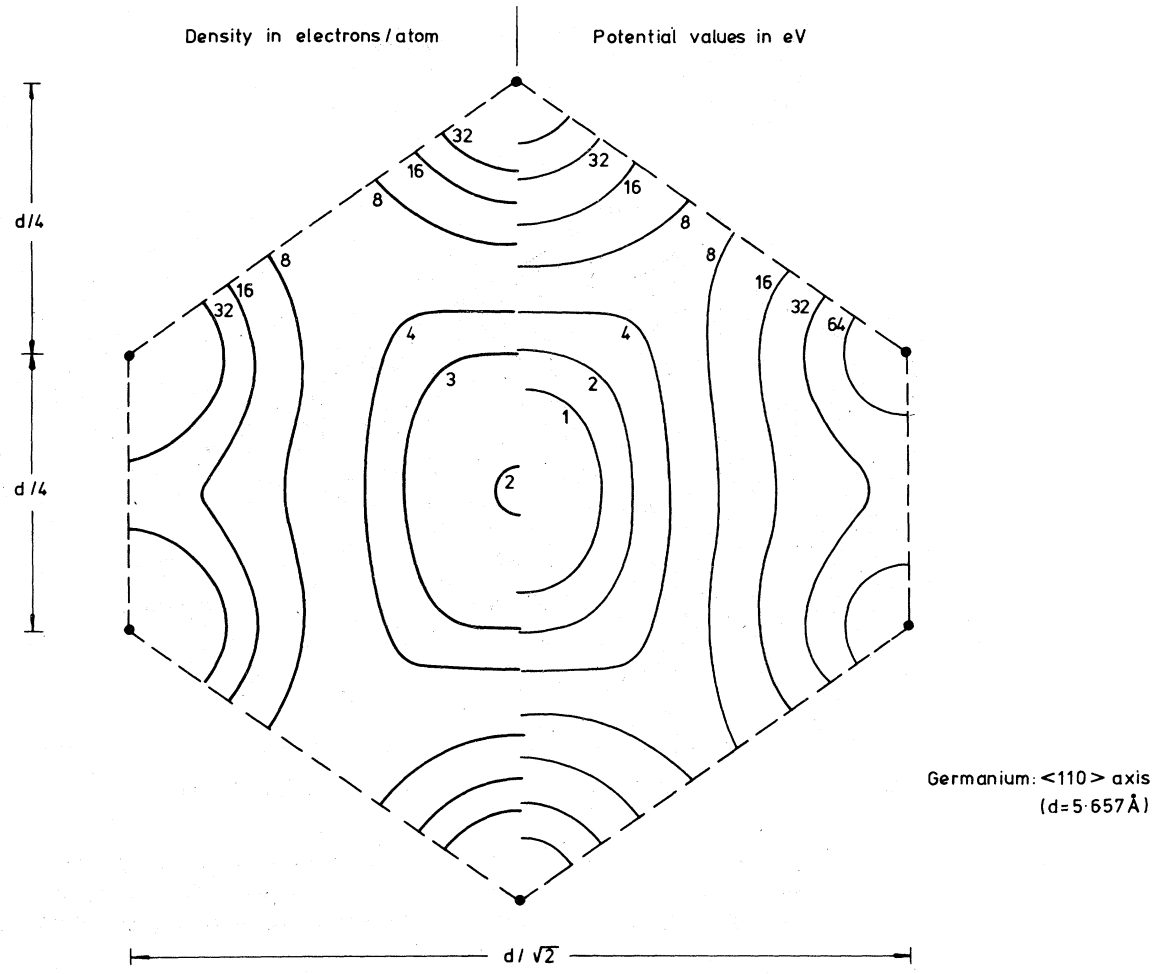

FIG. 9. The same as Fig. 7, for the {110} transverse plane in germanium.

$\langle Z_{1oc} \rangle$ for the two flat distributions. The results of the continuum model calculations for $\langle Z_{1oc} \rangle$ and Z_{axis} are presented in Table I for the $\langle 110 \rangle$ and $\langle 111 \rangle$ directions in silicon and germanium. The estimates for $\langle Z_{1oc} \rangle$ deduced by the use of Eq. (13) applied to our published $R_{\langle hkl \rangle}$ measurements with α particles are also presented in Table I, where they are seen to be entirely compatible with the calculated values.

D. Dechanneling

A particle penetrating into the crystal will become dechanneled when its transverse energy exceeds the critical value $E\psi_c^2$, where we take $\psi_{1/2}$ (B) to be a measure of ψ_c. The dechanneling length will depend on the rate of change of $E_\perp$, which will be determined by electronic multiple scattering, fluctuations in the interatomic repulsion due to thermal motions of the target atoms and by the damping effect due to the finite stopping power. Bjorkquist *et al.*[19] investigated these effects for 1.5 MeV protons channeled in silicon and found for axial channeling that the electronic contribution dominates for low $E_\perp$, and that thermal atomic vibrations became important for $E_\perp > 0.6E\psi_1^2$; the damping effect was relatively small. Owing to the rapid increase of $dE_\perp/dx$ with $E_\perp$ due to thermal vibrations, it is possible, at 1.5 MeV, to adopt the steady-state increase approximation and thus to deduce the dechanneling without consideration of the diffusive spreading due to electron scattering. At 160 MeV, both thermal vibrations and damping are small in comparison with the electron scattering term. Thus, we may adopt Feldman's result[20] for planar channeling where diffusive spreading was found to produce an exponential variation of channeled fraction with depth x,

$$f_{ch}(x) = \text{const} \times \exp(-0.693x/x_{1/2}) . \quad (22)$$

We can relate $x_{1/2}$ to the electron multiple scattering angle Ω and the critical channeling angle

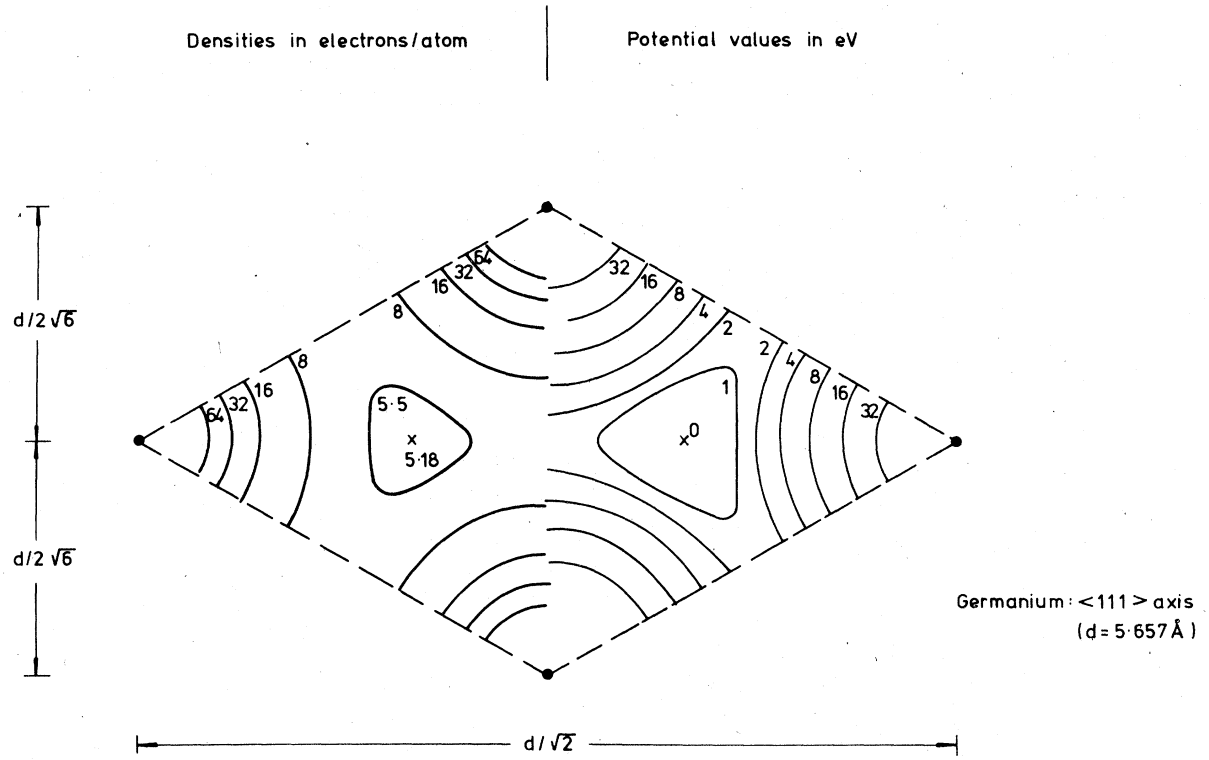

FIG. 10. The same as Fig. 8, for the {111} transverse plane in germanium.

ψ_c in the following approximate manner. In the absence of dechanneling the distribution in angular deviation ψ due to multiple scattering is nearly Gaussian,

$$P(\psi)2\pi\psi d\psi=(2\psi d\psi/\Omega^2)\exp(-\psi^2/\Omega^2)\,, \tag{23}$$

and a characteristic length X can be defined by the condition that the fraction of particles with $\psi>\psi_c$ should be $\frac{1}{2}$. However, this fraction refers to particles with $\psi>\psi_c$ at penetration depth X, whereas in channeling, particles are lost immediately as ψ exceeds ψ_c. A first order estimate of this loss can be obtained by recognizing that once a particle attains $\psi=\psi_c$ at any $x<X$ in the nonchanneling situation, it will have an equal chance of continuing to greater or lesser values of ψ. Thus, the loss of particles by dechanneling is about double the number indicated by the multiple-scattering formula, and we obtain $x_{1/2}$ from

$$\exp[-\psi_c^2/\Omega^2(x_{1/2})]=\tfrac{1}{4}\,.$$

Substituting for Ω, we find

$$x_{1/2}=\frac{\psi_c^2}{\ln 4(m/M_1E)S_eN\langle Z_{\rm loc}\rangle}\,, \tag{24}$$

where

$$S_e=(4\pi Z_1^2e^4/mv^2)\ln(2mvv_F/\hbar\omega)\,.$$

Estimating ψ_c by using the Barrett formula and substituting for the fixed quantities gives the

TABLE I. String-potential model electron densities in axial channels (electrons/atom).[a]

Crystal	Axis	$E\psi_{1/2}^2(B)/Z_1$ (eV)	$Z_{\rm axis}$	$\langle Z_{\rm loc}\rangle$	Z_R
Si	⟨110⟩	81.3	1.77	4.8 ± 0.6	4.9 ± 0.4
	⟨111⟩	66.4	3.61	6.0 ± 0.5	7.0 ± 0.4
Ge	⟨110⟩	136.6	1.97	8.7 ± 1.3	9.1 ± 0.6
	⟨111⟩	111.5	5.92	10.5 ± 1.1	13.0 ± 0.5

[a] $\langle Z_{\rm loc}\rangle$ results refer to a temperature of 293 °K; Z_R are densities deduced from $R_{\langle hkl\rangle}$ and Eq. (13).

following dechanneling lengths at 293 °K:

$$x_{1/2}(\mathrm{Si}) = 0.064 E/Z_1\langle Z_{1oc}\rangle L_e , \tag{25}$$

$$x_{1/2}(\mathrm{Ge}) = 0.121 E/Z_1\langle Z_{1oc}\rangle L_e , \tag{26}$$

where $x_{1/2}$ is in mm, E is in MeV, and $L_e = \ln(2mvv_F/\hbar\omega) \approx 5$ for 160 MeV α particles. At relativistic energies E is to be replaced by $\frac{1}{2}pv$ and v in L_e by $v/(1-\beta^2)^{1/2}$. The above result is not precise; a normalizing factor close to unity may be needed.

E. Trajectory spread

In channeling experiments the statistical energy loss straggling has occasionally been taken[21] to be a good determinant of $\langle Z_{1oc}\rangle$, but this is only correct if full account is also taken[8] of the phenomenon of trajectory spread. For channeling in targets with thickness small compared with the transverse oscillation wavelength λ, for which the electron multiple scattering will also be small, it is clear that the spread in energy loss will be directly proportional to the difference $Z_{1oc}(E_{\perp,\max}) - Z_{\mathrm{axis}}$, corresponding to the width of the $E_\perp$ distribution; the statistical spread will be small in comparison and will determine only the shape of the energy loss distribution around the low-energy-loss region corresponding to $E_\perp = 0$. For very thick targets where the $E_\perp$ diffusion ensures that all particles explore the accessible regions of the channel equally the trajectory spread will be very small and the statistical straggling will be dominant. For targets of intermediate thickness t the trajectory spread will be related to the strength of the $E_\perp$ diffusion, for which the dechanneling half length is an appropriate measure. Intuitively, we expect the trajectory spread FWHM W to vary inversely with the number of dechanneling half lengths $t/x_{1/2}$, i.e.,

$$W \sim \frac{\Delta E(Z_{\max}) - \Delta E(Z_{\mathrm{axis}})}{t/x_{1/2}} . \tag{27}$$

From our calculations of $Z(E_\perp)$, the stopping-power contribution from valence electrons and, in anticipation of the results of the dechanneling measurements, setting $t/x_{1/2} \sim 3$ shows that W is of the order of 15% of the channeled energy loss and is comparable with the statistical spread observed in the present work.

Our analysis of the energy-loss distributions for channeled particles utilizes the Landau-Vavilov formulation[14] as used for the random loss distributions. Trajectory spread is taken into account by convoluting the statistical-loss distribution and a Gaussian of width W. If $\langle Z_{1oc}\rangle$ is known, then W can be determined empirically. The Landau-Vavilov formulation determines $\langle \Delta E\rangle$ and $\langle \Delta E^2\rangle$ simultaneously for random loss and is not directly applicable to channeling where the proportion of close and distant collisions is different; only the former produce statistical fluctuations. To use the formulation for channeling, $\langle Z_{1oc}\rangle$ should be substituted for Z_2, the random-loss logarithmic term $\ln(2mv^2/I)$ retained and the indicated mean energy loss supplemented as necessary to fit the data by adding a term attributable to an excess contribution from distant collisions.

IV. DATA REDUCTION

A. Dechanneling

An estimate of the fully channeled fraction of the transmitted particles, and hence $x_{1/2}$, has been obtained from each singles spectrum taken with the silicon detector in its aligned position. The fully channeled particles can be distinguished from dechanneled particles by reference to the corresponding coincidence spectrum. The lack of a random peak on the two-proton-coincidence spectra can probably be attributed to the particular care taken with collimator and detector alignment for the proton work which was the main topic of the experiment. It is obviously necessary to distinguish particles dechanneled early in their passage through the crystal from those which were never channeled. For a parallel beam incident on the crystal the fraction not becoming channeled is very small,[12] being of the order of 18.8 Ndu_1^2 (a few percent). More important is the effect of beam divergence. The beam divergence at the collimator preceding the crystal was very small (<0.03° full width at base), but between the collimator and the crystal was an 8-μm vacuum window, 1 cm of air, and a 5-μm aluminum light-tight window—a total of 3 mg/cm^2 of material—which introduce an rms multiple-scattering angle comparable with ψ_1. The fraction of the particles which were initially accepted for channeling can now be calculated assuming a Gaussian multiple-scattering distribution and a channeling acceptance angle $\psi_a = \psi_{1/2}(B) = 0.88\psi_1$. Typically we find 50% of the particles to be so accepted. Interestingly, provided rechanneling is negligible, the singles spectra demand $\psi_a > 0.8\psi_1$, otherwise the calculation shows fewer particles initially channeled than are present as partially channeled events. The channeling fraction f_{ch}, the ratio of the fully channeled particles to the total initially channeled, is quoted for each spectrum in Table II, together with the deduced value of $x_{1/2}$(expt) and the theoretical estimate $x_{1/2}$(calc) deduced from Eq. (25)

TABLE II. Dechanneling lengths; theory and experiment.[a]

Target	Particle	Energy (MeV)	L_e	Axis	f_{ch}	$x_{1/2}$ (expt) (mm)	$x_{1/2}$ (calc) $\langle Z_{loc}\rangle = 4$
Si	p	158.5	5.30	⟨110⟩	0.19 ± 0.06	0.38 ± 0.07	0.44
				⟨111⟩	0.16 ± 0.04	0.28 ± 0.04	
	d	81.5	4.77	⟨110⟩	0.13 ± 0.04	0.31 ± 0.04	0.27
				⟨111⟩	0.13 ± 0.04	0.25 ± 0.04	
	α	160.0	4.77	⟨110⟩	0.08 ± 0.02	0.25 ± 0.02	0.26
				⟨111⟩	0.08 ± 0.02	0.20 ± 0.02	
	p	38.9	4.75	⟨111⟩		0.12 ± 0.02	0.13
Ge	α	160.0	4.79	⟨110⟩			0.50
	p	700	5.77	⟨110⟩			3.80
	π^+	1220	7.25	⟨110⟩			3.68

[a] Target thickness for silicon, $t = 0.739 \pm 0.006$ (⟨111⟩), 0.905 ± 0.007mm (⟨110⟩); $x_{1/2}$ (expt) $= -0.693\, t/\ln(f_{ch})$; Ge results for p and π^+ refer to 100°K (Ref. 7); Normalizing silicon $x_{1/2}$ (expt) to $x_{1/2}$ (calc) gives $Z_{loc,\langle 110\rangle} = 4.1 \pm 0.3$; $Z_{loc,\langle 111\rangle} = 5.4 \pm 0.4$; The choice of $\langle Z_{loc}\rangle = 4$ for calculating $x_{1/2}$(calc) is for convenience: in general $\langle Z_{loc}\rangle \neq 4$.

on the assumption $\langle Z_{1oc}\rangle = 4$. Fitting the experimental to the theoretical dechanneling lengths with $\langle Z_{1oc}\rangle$ as the fitting parameter yields $Z_{1oc,\langle 110\rangle} = 4.1 \pm 0.3$ and $Z_{1oc,\langle 111\rangle} = 5.4 \pm 0.4$. These densities are in fair agreement with the previous estimates, in Table I, and there appears to be little need to introduce a normalizing factor for Eq. (24).

Of particular interest is the dechanneling half-length measured by Acerbi *et al.*[18] for 38.9 MeV protons. The measured value was 0.12 mm, to which we assign an uncertainty of ±0.02 mm. Since Acerbi's work involved the use of a well-collimated beam, no multiple scattering, and their $x_{1/2}$ was essentially determined by target thicknesses less than 0.2 mm, we expect $\langle Z_{1oc}\rangle$ appropriate to their work to lie in the range $3.61 \leq \langle Z_{1oc}\rangle \leq 6.0 \pm 0.7$, i.e., to be rather less than found for our work.

Also shown in Table II are calculated values of $x_{1/2}$ for germanium for comparison with our previous experiment[6] and with that of Esbensen *et al.*[7] The quoted dechanneling lengths result from the use of $\langle Z_{1oc}\rangle = 4$; the actual values of $\langle Z_{1oc}\rangle$ are larger.

B. Stopping powers

The Landau-Vavilov energy-loss straggling distribution has been shown to give a good representation of random loss data taken with a wide range of particle types and energies in the intermediate energy region,[22] although the quality of the fits to the data have not in general been subjected to the customary statistical tests. In the present work we found it necessary to convolute each theoretical distribution with a Gaussian distribution with FWHM W. The random spectra in Figs. 11–16 were accordingly fitted using a three-parameter least-squares search routine in which the parameters were peak height H, energy-loss calibration (target thickness S being used for convenience), and FWHM spread W. Of the six random spectra only the ⟨110⟩ α-particle spectrum failed to be statistically acceptable, although the fit is visually satisfactory (see Figs. 11–16). The results of the analysis are shown in Table III. The Gaussian width W is in each case larger than the

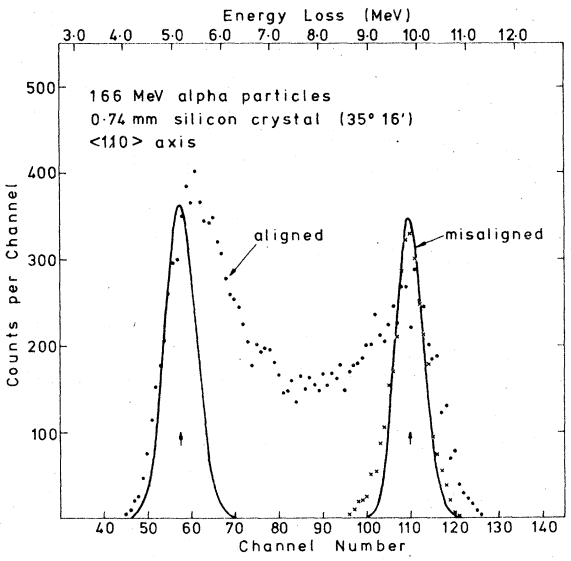

FIG. 11. The aligned (gated) spectrum and the misaligned (singles) spectrum for 160-MeV α particles incident close to the ⟨110⟩ direction of the silicon detector. The Landau-Vavilov energy-loss distributions are shown fitted to the data as discussed in the text. The arrows indicate the mean energy losses.

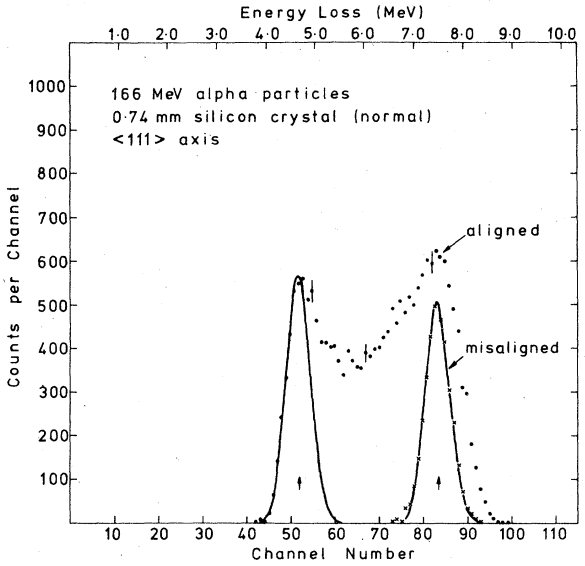

FIG. 12. Same as Fig. 11, for 166-MeV α particles and the ⟨111⟩ axis.

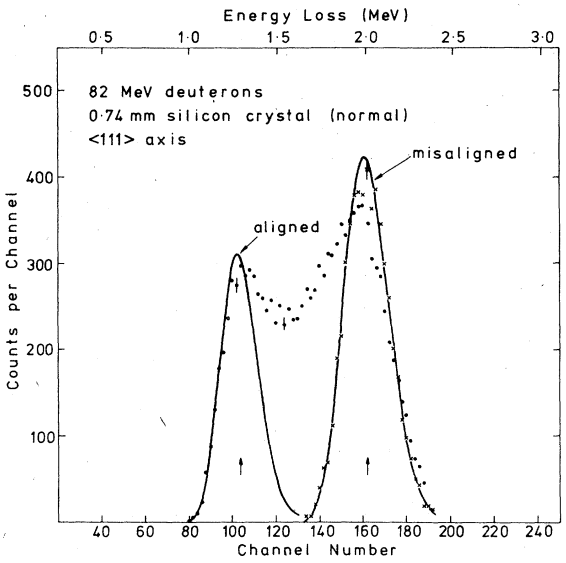

FIG. 14. Same as Fig. 11, for 82-MeV deuterons and the ⟨111⟩ axis.

value expected from the noise level alone (~30 keV), but additional contributions arise from the beam energy spread, from the correction needed for excess target thickness[15] (α-particle spectra only), and from the variation in target thickness over the lateral dimensions of the particle beam; even when aggregated these effects do not entirely explain the observed widths.

The least-squares fitting procedure was also applied to the channeled spectra, although there are a number of problems, both theoretical and experimental, which hindered this activity. Firstly, only that portion of each channeled spectrum falling on the low-energy side of the peak—and possibly including the peak—can be used for the analysis because this is where dechanneling effects will be least important. Secondly, there is the problem of selecting an effective target thickness for use in the analysis discussed in Sec. III E. Finally, it was expected that the

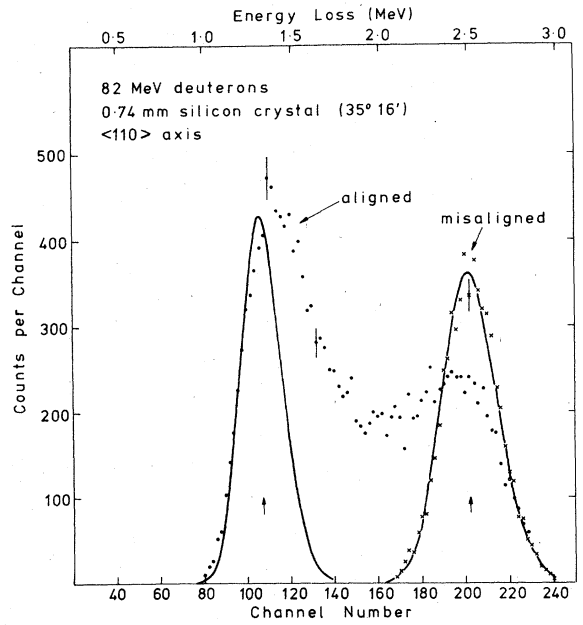

FIG. 13. Same as Fig. 11, for 82-MeV deuterons and the ⟨110⟩ axis.

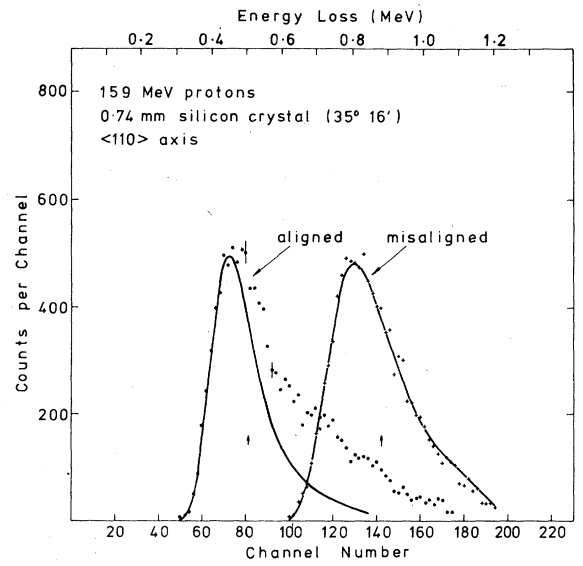

FIG. 15. Same as Fig. 11, for 159-MeV protons and the ⟨110⟩ axis.

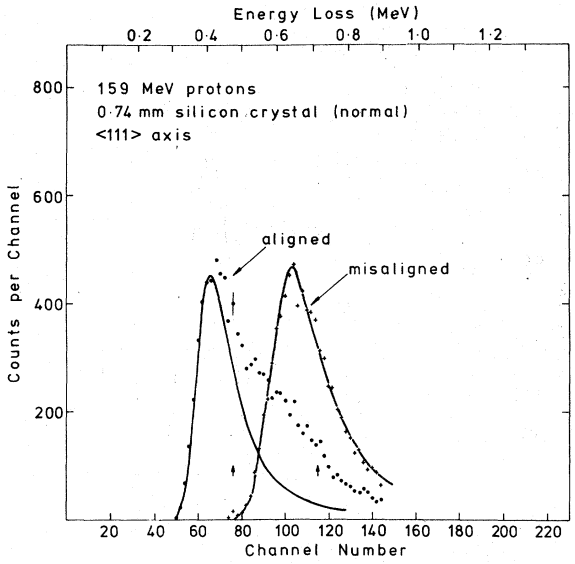

FIG. 16. Same as Fig. 11, for 159-MeV protons and the ⟨111⟩ axis.

width W of the Gaussian would be determined in a manner analogous to that used for the random spectra, but the additional contribution from trajectory straggle proved to be dominant.

The channeled spectra were analyzed for different assumed values of the effective target thickness: (i) the channeled energy loss was taken to be in simple proportion to the mean electron density so that the straggling calculation should fit energy loss and straggling simultaneously; (ii) the valence electron density distribution was taken to be uniform ($Z_{1oc} \simeq 4$) and the straggling calculated accordingly; the energy loss then had to be assumed to be supplemented by an additional distant collision contribution; (iii) the axial valence electron distribution was taken to be negligible so that there would be no straggling contribution for well-channeled particles (for protons only).

On purely statistical goodness-of-fit grounds, no observation can be made which permits an empirical choice to be made for $\langle Z_{1oc} \rangle$. For α particles or deuterons the question of selecting $\langle Z_{1oc} \rangle$ is unimportant because the Landau-Vavilov distribution is very nearly Gaussian—and a convolution of two Gaussians produces a third—so that the resulting mean energy loss $\Delta\overline{E}$, and hence $R_{\langle hkl \rangle}$, is obtained in a manner independent of the details of the calculation. On the other hand, the proton distributions are skewed so that a change in $\langle Z_{1oc} \rangle$ introduces a corresponding change in W and in $R_{\langle hkl \rangle}$. However, the discussion of Sec. III E provided a prescription for this difficulty that entailed determining $\langle Z_{1oc} \rangle$ either from calculation, Sec. III C or from the results of the (previous) α-particle measurements, Sec. III B. We adopt $Z_{1oc,\langle 110 \rangle} = 4.8 \pm 1.0$ and $Z_{1oc,\langle 111 \rangle}$

TABLE III. Results of least-squares analysis of energy-loss distributions.[a]

Particle	Axis	Ch/r	FWHM (keV)	W (keV)	$\langle Z_{loc} \rangle$	$\Delta\overline{E}$ (MeV)	$R_{\langle hkl \rangle}$
α	⟨110⟩	r	672	229	14.0	9.855	
		Ch	761	609	7.4	5.180	0.526
		Ch	855	800	3.7	5.167	0.524
	⟨111⟩	r	570	231	14.0	7.482	
		Ch	580	399	8.7	4.655	0.622
		Ch	628	500	4.2	4.620	0.618
d	⟨110⟩	r	372	199	14.0	2.513	
		Ch	279	154	7.4	1.331	0.530
		Ch	279	223	3.9	1.340	0.538
	⟨111⟩	r	298	105	14.0	2.013	
		Ch	248	105	9.0	1.291	0.641
		Ch	235	182	4.5	1.288	0.640
p	⟨110⟩	r	236	69	14.0	0.884	
		Ch	155	68	8.0	0.506	0.572
		Ch	121	91	3.4	0.469	0.530
		Ch	104	104	0.0	0.441	0.499
	⟨111⟩	r	205	64	14.0	0.713	
		Ch	130	35	9.2	0.432	0.658
		Ch	95	63	4.0	0.432	0.605
		Ch	80	80	0.0	0.404	0.567

[a] $\langle Z_{loc} \rangle$ is the valence-electron density assumed for the Landau-Vavilov straggling calculation. Final ratios $R_{\langle hkl \rangle}$ for protons were identified using $\langle Z_{loc} \rangle$ from Table I. Ch: channeled; r: random.

TABLE IV. Final experimental results for $R_{\langle hkl\rangle}$ in Si.

Expt	Particle	Energy (MeV)	Axis	$R_{\langle hkl\rangle}$
Previous work	α	160	$\langle 110\rangle$	0.499 ± 0.021
			$\langle 111\rangle$	0.615 ± 0.015
This work	α	160	$\langle 110\rangle$	0.534 ± 0.020
			$\langle 111\rangle$	0.625 ± 0.020
	d	81.5	$\langle 110\rangle$	0.533 ± 0.020
			$\langle 111\rangle$	0.643 ± 0.020
Best estimate	α,d		$\langle 110\rangle$	0.522 ± 0.012
			$\langle 111\rangle$	0.625 ± 0.010
This work	p	158.5	$\langle 110\rangle$	0.543 ± 0.020
			$\langle 111\rangle$	0.630 ± 0.020

$=6.5\pm1.0$, and since $R_{\langle hkl\rangle}$ for protons is found to vary linearly with $\langle Z_{1oc}\rangle$, we obtain $R_{\langle hkl\rangle}=0.543\pm0.010$ and $R_{\langle 111\rangle}=0.630\pm0.010$ (the errors referring only to $\delta Z_{1oc}=1.0$).

An important, but difficult, problem is that of assessing the uncertainties to be associated with the $R_{\langle hkl\rangle}$ values. The results quoted in Table III were derived from a particular set of data points from each spectrum; once the data set is defined the uncertainty involved in the fitting procedure is small. The main problem is thus to determine the uncertainty associated with the choice of data sets. Our preferred sets included the peaks of the distribution if it was clear that so doing would not broaden the distribution significantly. The choice of a reduced set (i.e., excluding points at the peak) does not necessarily result in a different set of fitting parameters. However, if the data set included only those points on the low-energy side of the spectrum below $\frac{2}{3}$ of the peak height, and a fit is forced with the peak reduced to $\frac{2}{3}$ its former value, then we find the ratios R reduced by $\delta R\sim0.04$. Alternatively, one could use the low-energy intercept as a reference point, assume W from the appropriate random spectrum, and take $Z_{1oc}=4$; this results in a reduction of $\delta R\sim0.03$. Ultimately, the assignment of uncertainties is a matter for enlightened judgement rather than of numerical assessment and we consider an allowance $\delta R\sim0.02$ to be reasonable.

The results quoted in Table III refer to mean particle energies which depend not only on particle but also on target orientation and whether random or channeling conditions apply. Small amendments are therefore needed to yield the stopping ratios relevant for very thin targets; our final results are presented in Table IV. The deuteron ratios are not significantly different from the α-particle ratios; this is the expected result since these ions possess the same v and E/M, so that only a Z_1^2 dependence in stopping power should be observed. The present α-particle data agree with the measurements obtained previously.[5] Accordingly, we determine our best estimates of $R_{\langle hkl\rangle}$ for α particles and deuterons as the average of the three sets. The proton ratios are not significantly larger than these best estimates and do not display the modest increases predicted in Sec. III B, although the uncertainties are such that no inconsistency can be claimed; it is noteworthy that larger ratios for protons can be obtained only by increasing $\langle Z_{1oc}\rangle$.

C. Trajectory spread

The W values for random energy loss are much greater than the 30 keV noise level, but the excess is largely due to factors proportional to the mean energy loss; the W values for channeling would therefore be expected to be about half the random values, whereas in practice they are comparable or greater (particularly for the α-particles spectra). As noted in Sec. III E, the large values observed for W can be attributed to a trajectory spread with an estimate for W of

$$W\approx\frac{\Delta E(\hat{Z})-\Delta E(Z_{axis})}{t/x_{1/2}}.$$

Since Eq. (12) shows $R_{\langle hkl\rangle}$ to be proportional to Z_{1oc}, we can rewrite this result as

$$\left(\frac{W}{\Delta\bar{E}}\right)_{calc}\approx\left(\frac{\hat{Z}-Z_{axis}}{14}\right)\frac{L_1}{L_2}\Big/\left[1-\left(\frac{14-Z_{1oc}}{14}\right)\frac{L_1}{L_2}\right]\frac{t}{x_{1/2}}$$
$$=\left(\frac{\Delta R}{R}\right)\Big/\left(\frac{t}{x_{1/2}}\right),\qquad(28)$$

where $L_1=\ln(2mvv_F/\hbar\omega)$ and $L_2=\ln(2mv^2/I)$. For very thin targets we should take $\hat{Z}=Z_{max}$ appropriate to $E(\max)=E\psi_{1/2}^2(B)$, but since dechanneling denudes the $E_\perp$ distribution of high-$E_\perp$ particles it appears more appropriate to assume $\hat{Z}$ to be defined by the flat $E_\perp$ distribution, giving the

TABLE V. Comparison of calculated and experimental values for W in Si.

Particle	Axis	$\Delta R/R$	$t/x_{1/2}$	$(W/\Delta\bar{E})_{\text{calc}}$	$(W/\Delta\bar{E})_{\text{expt}}$
α	⟨110⟩	0.539	3.6±0.3	0.15±0.02	0.16
	⟨111⟩	0.426	3.7±0.4	0.11±0.01	0.09
d	⟨110⟩	0.539	2.9±0.4	0.19±0.03	0.13
	⟨111⟩	0.425	3.0±0.5	0.14±0.02	0.11
p	⟨110⟩	0.469	2.4±0.5	0.20±0.04	0.14
	⟨111⟩	0.375	2.6±0.4	0.14±0.02	0.08

same $\langle Z_{1oc}\rangle$ as the result accepted in Table I. The value for W appropriate to channeling is not that value quoted in Table III, but rather the value obtained after subtracting (quadratically) half of the W value for random particles, thus taking into account noise, beam energy spread, etc. The experimental and calculated values for W/E are compared in Table V, from whence we obtain the satisfactory result

$$(W/\Delta\bar{E})_{\text{expt}} \approx (0.74\pm0.06)(W/\Delta E)_{\text{calc}}. \quad (29)$$

V. DISCUSSION

A. Relativistic measurements of $R_{\langle hkl\rangle}$

The measurement of $R_{\langle 110\rangle}$ in germanium for 700-MeV protons and 1200-MeV π^+ by Esbensen *et al.*[7] must be explained in terms of our simple theory. This very high-energy experiment differs in several features from the present work: (i) the germanium detector was cooled to 100°K so that $\psi_{1/2}(\text{B}) = 0.88\psi_1$; (ii) the relativistic formula, Eq. (13), must be used; (iii) the dechanneling length is not short compared with the detector thickness.

It is this last feature which is the most significant. For $x_{1/2} \gg t$ it would be appropriate to fit the energy-loss spectrum assuming an axial electron density Z_{axis} and discounting the trajectory spread convolution since there would be little or no diffusion in $E_\perp$ values. However since $x_{1/2}/t = p$ is only of the order 5 there will be few particles whioh travel along the entire length of the channel axis. The approximate trajectory spread can be estimated by identifying the dechanneling half-length with the penetration after which particles entering with $E_\perp = 0$ have acquired $E_\perp = E\hat{\psi}^2$, which is the maximum transverse energy associated with the flat $E_\perp$ distribution equivalent to the trapezoidal distribution in ψ defined by $\psi_{1/2}(\text{obs})$. The effective $\langle Z_{1oc}\rangle$ and trajectory spread $W(Z)$ associated with the particles contributing to the low-energy-loss portion of the Esbensen spectra are to be derived from a flat $E_\perp$ distribution of width $p^{-1}E\hat{\psi}^2$. We find $p = 4.5$, $\langle Z_{1oc}\rangle = 5.0\pm1.0$, and $W \sim 40$ keV. These values permit us to take account of energy-loss straggling and to obtain the values for $R_{\langle 110\rangle}$ for germanium quoted in Table VI. These values are significantly larger than those deduced assuming the low-energy intercept to give the best-channeled ratios directly. However, the ratios we now deduce as being appropriate for best-channeled particles (i.e., replacing $\langle Z_{1oc}\rangle$ by Z_{axis}) are not very different from the values deduced (incorrectly) from the intercepts.

B. Comparison of experiments with theory

The results of the high-energy channeling experiments are summarized in Table VI and compared with predictions from the simple theory expressed in Eq. (13) with the theory of Dettmann and that of Golovchenko and Esbenson (GE). Only Eq. (13) can be compared directly with the experimental measurements. As seen from the final two columns of Table VI, the simple theory is quite remarkably successful. The theory of

TABLE VI. Theoretical values for $R_{\langle hkl\rangle}$ compared with experiment.[a]

Expt	Crystal	Axis	Eq. (13) (Z_{axis})	GE	Eq. (13) (Z_{val})	Dettmann	Eq.(13) (Z_{loc})	Expt
160 MeV α's	Si	⟨110⟩	0.33	0.34	0.45	>0.52	0.49±0.03	0.522±0.012
		⟨111⟩	0.43	0.51	0.45	0.57	0.56±0.03	0.625±0.010
160 MeV α's	Ge	⟨110⟩	0.18	0.21	0.24	0.35	0.37±0.03	0.375±0.015
		⟨111⟩	0.29	0.33	0.24	0.40	0.41±0.03	0.481±0.012
700 MeV p	Ge	⟨110⟩	0.33	0.28			0.39±0.02	0.38 ±0.03
1220 MeV π^+	Ge	⟨110⟩	0.37				0.43±0.02	0.41 ±0.03

[a] For 700-MeV p, 1220-MeV π^+; we take $\langle Z_{\text{loc}}\rangle = 5.0\pm1.0$.

TABLE VII. Experimental $R_{\langle hkl\rangle}$ values corrected for valence-electron density.

Expt	Crystal	Axis	Expt(Z_{axis})	GE	Expt(Z_{val})	Dettmann
160 MeV α's	Si	⟨110⟩	0.36±0.03	0.34	0.48±0.03	>0.52
		⟨111⟩	0.50±0.03	0.51	0.51±0.03	0.57
160 MeV α's	Ge	⟨110⟩	0.18±0.03	0.21	0.24±0.03	0.35
		⟨111⟩	0.36±0.03	0.33	0.31±0.03	0.40
700 MeV p	Ge	⟨110⟩	0.32±0.03	0.28		
1220 MeV π^+	Ge	⟨110⟩	0.35±0.03			

Dettmann assumed a valence electron distribution that is uniform, with $Z_{val}=4$ electrons/atom; the Dettmann predictions are all significantly larger than the results of using $Z_{loc}=4$ in Eq. 13. The theory of Golovchenko and Esbenson recognizes that there is a dependence of the channeled stopping power on the electron density distribution and their predictions refer to the best-channeled particles, i.e., $Z_{loc}=Z_{axis}$. The agreement between Eq. (13) using $\langle Z\rangle=Z_{axis}$ and the GE predictions is quite close. Superficially the theory of Dettmann is a better fit to the data than is that of GE but it is now apparent that the data should not be compared directly with either. Having shown that Eq. (13) gives a fair representation of the calculations of GE and of the raw data it is perhaps most appropriate to use Eq. (13) to correct the experimental results such that the two theoretical approaches may be confronted with relevant data. This is done in Table VII. Not surprisingly, the theory of GE is seen to fit the corrected experimental results extremely well whereas that of Dettmann produces serious overestimates.

The theory of Dettmann is relatively transparent so it is of interest to investigate why its predictions are unduly high. In the high-velocity limit Dettmann's theory gives for $R_{\langle hkl\rangle}$ an approximate, channel independent, result

$$R=[Z_{val}+\tfrac{1}{2}(Z_2-Z_{val}-Z_{core})]/Z_2,$$

where Z_{core} refers to the core electrons (2 for silicon, 10 for germanium) that are not excited by distant collisions, whereas the outer electrons are excited just as effectively for channeling as for random trajectories. The distinction between core and outer electrons is based on detailed calculations concerning the impact-parameter dependence of the various orbitals. The feature of Dettmann's calculations giving most concern is the finding that, provided the bound electrons contribute to the distant collision energy loss, they should do so as effectively as the valence electrons which are not effectively bound at all; i.e., Dettmann requires $L_{c,d}$ [of Eq. (9)] should be of similar magnitude to $\ln(v/v_F)$, whereas from Sec. III B it is found that $L_{c,d}$ is nearly one order of magnitude smaller. The surprising feature of Dettmann's calculations is not that the ratio R should be high, but that his random stopping power S_r should be so nearly correct. Evidently Dettmann underestimates the core electron close collision contribution to random energy loss to the same extent that he overestimates the distant collision term (in Dettmann's terminology he has the result $S_{r,1}\approx S_{r,2}$).

VI. SUMMARY

We have found a simple expression can be formulated for $R_{\langle hkl\rangle}$, which gives a very satisfactory fit to the available data in the high-velocity limit, including relativistic velocities, provided an averaging procedure is invoked to determine the average electron density in the channel. It is evident that the term "best-channeled" expresses a simplification convenient for theory but one which is not in general susceptible to experimental demonstration.

In previous experiments $R_{\langle hkl\rangle}$ was determined for 160 MeV α particles in silicon and germanium using a technique in which the full beam energy was recorded. The results were superficially in good agreement with the theory of Dettmann but not with that of GE. Because of the large energy spread in the incident beam it was possible to obtain no useful information other than the ratio $R_{\langle hkl\rangle}$. The present work using a thin $\Delta E/\Delta x$ detector confirmed the previous $R_{\langle hkl\rangle}$ measurement, but also provided information on dechanneling and trajectory spread, which led to the appreciation that an electron density averaging procedure was needed. As a consequence it is now understood that Dettmann's theory gives inadequate estimates of the core-electron local and distant energy loss contributions and overestimates the stopping ratio $R_{\langle hkl\rangle}$, whereas the calculations of GE are probably rather good.

The relativistic energy measurements of Esbensen *et al.* were observed to be in good agreement with predictions of GE. However, their assertion that the low-energy intercept gives the best-channeled stopping power is incorrect and it is merely fortuitous that a full investigation involving statistical energy-loss straggle, trajectory spread and a correction for the averaged electron density should yield a result which remains close to the low-energy intercept result.

Nowhere, here or in the literature, is a discussion provided on the effect produced by non-axial-channeling trajectories on the bound-electron distant collision excitation contribution: the necessary corrections are evidently small.

---

[1]H. Bethe, Ann. Physik 5, 325 (1930).
[2]F. Bloch, Ann. Physik 16, 285 (1933).
[3]K. Dettmann, Z. Physik A 272, 227 (1975).
[4]J. Golovchenko and H. Esbensen, Nucl. Instrum. Methods 123, 137 (1976)-abstract only; H. Esbensen and J. Golovchenko, Nucl. Phys. A 298, 382 (1978).
[5]O. N. Jarvis, A. C. Sherwood, C. Whitehead, and M. W. Lucas, Phys. Rev. B 16, 3880 (1977).
[6]O. N. Jarvis, A. C. Sherwood, C. Whitehead, and M. W. Lucas, J. Phys. C 11, 2923 (1978).
[7]H. Esbensen, O. Fich, J. A. Golovchenko, K. O. Nielsen, E. Uggerhoj, C. Vraast-Thomsen, G. Charpak, S. Majewski, F. Sauli, and J. P. Ponpon, Nucl. Phys. B 127, 281 (1977).
[8]J. D. Melvin and T. A. Tombrello, Rad. Eff. 26, 113 (1975).
[9]A. Desalvo and R. Rosa, J. Phys. C 10, 1595 (1977).
[10]H. Bichsel and C. Tschalar, Nucl. Data, Sect. A 3, 343 (1967).
[11]O. N. Jarvis, A. C. Sherwood, C. Whitehead, and M. W. Lucas, Rad. Eff. 36, 215 (1978).
[12]D. S. Gemmell, Rev. Mod. Phys. 46, 129 (1974).
[13]D. Pines, Elementary Excitations in Solids (Benjamin, New York, 1964).
[14]P. V. Vavilov, Sov. Phys. JETP 5, 749 (1957); S. Seltzer and M. Berger, NAS-NRC 1133, 187 (1964).
[15]C. Tschalär, Nucl. Instrum. Methods 61, 141 (1968).
[16]J. Lindhard, Mat. Fys. Medd. Dan. Vid. Selsk. 34, No. 14 (1965).
[17]J. H. Barrett, Phys. Rev. B 3, 1527 (1971).
[18]E. Acerbi, C. Birattari, B. Candoni, M. Castiglioni, and C. Succi, Nuovo Cimento 29, 257 (1975).
[19]K. Bjorkquist, B. Cartling, and B. Domeij, Rad. Eff. 12, 267 (1972).
[20]L. C. Feldman, B. R. Appleton, and W. L. Brown, BNL Report No. BNL-50083, 1968 (unpublished), p. 58.
[21]B. R. Appleton, C. Erginsoy, and W. M. Gibsen, Phys. Rev. 161, 330 (1967).
[22]H. D. Maccabee, M. R. Raju, and C. A. Tobias, Phys. Rev. 165, 469 (1968).